

Magnetotransport in disordered delta-doped heterostructures

V. Tripathi^{1,2} and M. P. Kennett³

¹ *Theory of Condensed Matter Group, Cavendish Laboratory,
Department of Physics, University of Cambridge,
J. J. Thomson Avenue, Cambridge CB3 0HE, United Kingdom*

² *Department of Theoretical Physics, Tata Institute of Fundamental Research, Homi Bhabha oad, Mumbai 400005, India and*

³ *Physics Department, Simon Fraser University,
8888 University Drive, Burnaby, BC, V5A 1S6, Canada*

(Dated: November 13, 2017)

We discuss theoretically how electrons confined to two dimensions in a delta-doped heterostructure can arrange themselves in a droplet-like spatial distribution due to disorder and screening effects when their density is low. We apply this droplet picture to magnetotransport and derive the expected dependence on electron density of several quantities relevant to this transport, in the regimes of weak and moderate magnetic fields. We find good qualitative and quantitative agreement between our calculations and recent experiments on delta-doped heterostructures.

PACS numbers: 73.20.-r, 05.60.-k, 73.40.Gk, 75.47.-m

I. INTRODUCTION

Delta doping of semiconductor heterostructures has a history of leading to new and interesting physical phenomena, such as the fractional quantum Hall Effect.¹ This new physics has come from increasing the mobility of doped electrons by minimizing the disorder they feel due to the spatial separation between the dopants and the electrons. While spatial separation reduces the magnitude of fluctuations in the potential due to dopant atoms, it is well known that disorder due to the random positions of donors in the delta-doped layer has important consequences for the transport properties of heterostructures. Recent efforts have attempted to gain a clearer experimental picture of the nano-scale distribution of electronic states in two dimensional electron gases (2DEGs).^{2,3,4,5} Such electronic inhomogeneity on the nano-scale is believed to be important for transport in a wide variety of strongly correlated electronic materials.^{6,7,8}

A step towards a more systematic understanding of the effect of disorder on transport properties has been taken in recent experiments on delta-doped devices by Baenninger *et al.*^{9,10} where a series of small devices was fabricated in which the distance between the dopant layer and the 2DEG was varied in a controlled way. Some of these devices show very interesting resistance effects in a magnetic field. In particular, the dependence of the magnetoresistance on electron density has been suggested as evidence for charge density wave formation.¹⁰

In this paper, we argue that the observations of Ghosh *et al.*^{10,11,12,13} are a manifestation of charge droplet formation in a 2DEG. To justify this point of view, we analyze the charge distribution in a disordered 2DEG due to a delta doped layer, to demonstrate that in the devices of interest, the charge distribution likely consists of droplets of charge that sit in minima of the screened disorder potential. It is well known theoretically that the charge distribution in delta-doped heterostructures should have a droplet-like structure at low electron density.^{14,15} There

has also been recent interest in electron droplets in the vicinity of the 2D metal insulator transition,^{16,17} but relatively little attention has been paid to transport in insulating samples in a magnetic field (with the exception of Efros and co-workers^{18,19,20}).

We derive expressions for the physical parameters of electron droplets in the non-linear screening regime that is relevant to the experiments of interest here, and then apply this picture to describe the transport in these devices. We observe that our picture implies that the tunneling between droplets decreases as a function of magnetic field in a manner that is consistent with experiment. The picture for the magnetoresistance at small fields is along the lines of that proposed by Glazman and Raikh,²¹ while at larger fields, the magnetoresistance crosses over to the behavior expected by Shklovskii and Efros.^{22,23} These approaches^{21,22,23} provide the magnetic field dependence of the resistance, but the picture of electron droplets yields non-trivial predictions for the dependence of resistance on parameters other than magnetic field, such as electron and dopant densities. In particular we show that in the regime of magnetic fields where the resistivity ρ varies with magnetic field B as $\rho(B) \propto \exp[\alpha B^2]$, that $\alpha \propto n_e^{-\frac{3}{2}}$, where n_e is the electron density in the 2DEG, even though the average tunneling distance between droplets is much larger than the average inter-electron spacing. We also expect α to be temperature-independent at low temperatures, as observed in experiment.

This paper is structured as follows: in Sec. II we introduce our model for the delta doped heterostructure and elucidate the mechanism by which electron droplets form, then characterize how their properties depend on sample parameters. In Sec. III we discuss the expectations for magnetotransport, based on the droplet picture, and compare the implications with actual transport measurements. Finally, in Sec. IV we conclude and discuss the implications of our results for experiment.

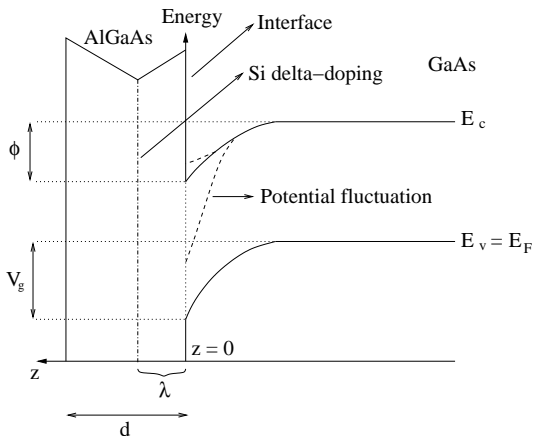


Figure 1: Bandstructure of the heterostructure indicated by bold solid lines. The 2DEG is formed at the interface $z = 0$ of AlGaAs and GaAs. The dashed lines indicate the random positions of the bottom of the conduction band in the 2DEG; the randomness arises from a spatially nonuniform distribution of δ -dopants. The potential ϕ at the interface is due to the gate voltage V_g , the ionized dopants' potential and screening by conduction electrons in the interface. E_c and E_v are the conduction and valence band energies, respectively, in bulk GaAs and E_F is the Fermi energy.

II. MODEL

In this section we introduce the physical situation that we are interested in, and the model we have of this system. We then derive in detail how disorder and screening effects give rise to a droplet-like electron density distribution in the 2DEG, and give the physical parameters of the electron droplets. We finally present a brief summary of the electron droplet picture.

A. Main parameters

The physical situation and several of the relevant parameters for the physics we will consider in more detail later are summarized in Fig. 1.

There are two classes of parameters that control the physics in the devices of interest: those that are intrinsic to GaAs, and those that can be varied experimentally, through fabrication of a device, or use of a gate. The properties that are intrinsic to GaAs are $\kappa = 12.9$, the dielectric constant of the GaAs or AlGaAs dielectric, and $m = 0.067m_e$, the effective electron mass in GaAs, which imply a Bohr radius for electrons in the 2DEG of $a_B = 4\pi\kappa\epsilon_0\hbar^2/me^2 \simeq 10$ nm. The following properties can be tuned in experiments:

1. d , the distance between the gate electrode and the 2DEG. Experimentally, $d \approx 300$ nm.
2. λ , the distance between the δ -doping layer from the 2DEG. $\lambda = 10 - 80$ nm. The typical λ used in our calculations is 50 nm.

3. $n_d \sim 10^{12} \text{ cm}^{-2}$, the density of dopants in the δ layer.
4. $n_e \sim 10^{11} \text{ cm}^{-2}$, the average density of electrons in the 2DEG in a typical sample. This will be the typical value in our calculations. Some samples have lower electron densities, $n_e \sim 10^{10} \text{ cm}^{-2}$.
5. V_g , the voltage at the gate electrode, which is metallic.

In our theoretical treatment, we always assume that $d \gg \lambda$, and $n_d \gg n_e$. The dielectric constants for GaAs and AlGaAs are also assumed to be the same without loss of generality.

B. Electron droplet formation in a 2DEG

Our discussion follows similar lines to the work of Gergel' and Suris,¹⁴ who considered the formation of electron droplets in a 2DEG when the average position of the bottom of the conduction band (see Fig. 1) is above the Fermi energy E_F . However, our results differ qualitatively from Ref. 14, and these differences are essential for connecting our results with experiment. Hence we present the effect of various experimentally relevant parameters on the properties of the droplets in some detail.

We assume that the donor positions are uncorrelated, and distributed with a white-noise Gaussian distribution, and that the donors are ionized after compensating the band-bending field, which provides the electrons for the two dimensional electron gas. We ignore effects due to incomplete and weak ionization.²⁴ For a mean δ -doping density of $n_d = 10^{12} \text{ cm}^{-2}$ and a 2DEG-dopant layer separation of $\lambda = 50$ nm, a complete ionization of the donors corresponds to a compensating potential $V_{\text{comp}} = e\lambda n_d / (\kappa\epsilon_0) \sim 1$ V. Random fluctuations in the dopant potential cause the bottom of the conduction band in some regions of the 2DEG to lie below E_F ; this leads to the appearance of electron droplets. In the rest of our discussion, we consider the potential ϕ in the 2DEG after subtracting the compensating potential. Charge fluctuations about the mean can be of either sign. We also assume that the chemical potential is uniform across the sample.

The charge density $\rho(z, \mathbf{r})$ in the AlGaAs region is

$$\rho(z, \mathbf{r}) = en(\mathbf{r})\delta(z - \lambda), \quad (1)$$

where $n(\mathbf{r}) = n_+(\mathbf{r}) - n_-(\mathbf{r})$ is the surface charge density in the δ -layer and \mathbf{r} is a two-dimensional vector in the δ -doping plane. The subscripts \pm denote the sign of the charge fluctuation. The spatial distribution of the dopant atoms satisfies

$$\langle n(\mathbf{r})n(\mathbf{r}') \rangle - \langle n \rangle^2 = n_d\delta(\mathbf{r} - \mathbf{r}'), \quad (2)$$

and $n_d = \langle n_+ \rangle + \langle n_- \rangle$ is the total surface charge density of *both* polarities in the δ -layer. The dopant atoms create a fluctuating potential $\phi(\mathbf{r})$ in the 2DEG,

$$\phi(\mathbf{r}) = V_{\text{comp}} + \frac{1}{4\pi\epsilon_0\kappa} \int d\mathbf{r}' \int_0^d dz \{ \rho(z, \mathbf{r}') - en_e [\phi(\mathbf{r}')] \delta(z) \} \langle \delta\phi^2 \rangle = \frac{n_d e^2}{8\pi\kappa^2 \epsilon_0^2} \left\{ \ln \left[\frac{4d^2}{\lambda(2d-\lambda)} \right] \right. \\ \left. \times \left[\frac{1}{\sqrt{(\mathbf{r}-\mathbf{r}')^2 + z^2}} - \frac{1}{\sqrt{(\mathbf{r}-\mathbf{r}')^2 + (2d-z)^2}} \right] \right. \quad (3) \\ \left. - 2 \ln \left[\left(\frac{\lambda^2 + R_c^2}{(2d-\lambda)^2 + R_c^2} \right)^{1/4} + \left(\frac{(2d-\lambda)^2 + R_c^2}{\lambda^2 + R_c^2} \right)^{1/4} \right] \right\}. \quad (6)$$

In Eq. (3), $n_e[\phi(\mathbf{r}')]$ is the electron charge density in the 2DEG and the first and second terms under the square root signs represent direct and image contributions from the charge distribution respectively. The position of the image charges is to the left of the metallic gate electrode $z = d$ in Fig. 1.

When the gate voltage V_g is small, the number of electrons n_e at the interface will be small. Let us first estimate the mean square value of the potential fluctuations, $\langle \delta\phi^2 \rangle$, at the interface by ignoring screening effects of finite electron density, n_e . Using Eqs. (2) and (3) one has

$$\langle \delta\phi^2 \rangle = \frac{2\pi n_d e^2}{(4\pi\kappa\epsilon_0)^2} \int dr r \left[\frac{1}{\sqrt{r^2 + \lambda^2}} - \frac{1}{\sqrt{r^2 + (2d-\lambda)^2}} \right]^2 \\ = \frac{n_d e^2}{8\pi\kappa^2 \epsilon_0^2} \ln \left[\frac{4d^2}{\lambda(2d-\lambda)} \right]. \quad (4)$$

When the gate voltage V_g is increased, the bottom of the conduction band approaches the Fermi energy E_F . If potential fluctuations due to the dopants are such that in some regions of the interface, the bottom of the conduction band now lies below E_F , a finite $n_e(\mathbf{r})$ will be found at such places (see Fig. 1).

Next we estimate the effect of screening on the mean square fluctuation $\langle \delta\phi^2 \rangle$ due to a local electron density $n_e(\mathbf{r})$. Consider a region of size R in the δ -layer. From Eq. (2), one can estimate the magnitude of fluctuations of $n(\mathbf{r})$ in this region:

$$\langle \delta n^2(R) \rangle = \frac{1}{\pi R^2} \int_0^R d\mathbf{r}' \langle (n(\mathbf{r})n(\mathbf{r}')) - \langle n \rangle^2 \rangle = \frac{n_d}{\pi R^2}. \quad (5)$$

Thus $\sqrt{\langle \delta n^2(R) \rangle} \sim n_d^{1/2} / \pi^{1/2} R$ is the characteristic fluctuation of the dopant charge density. If the local electron charge density, $n_e(\mathbf{r})$, exceeds $\sqrt{\langle \delta n^2(R) \rangle}$, then potential fluctuations due to these fluctuations in charge density will be screened by a redistribution of the electronic charge n_e . If the local electron charge density is much less than $\sqrt{\langle \delta n^2(R) \rangle}$, then potential fluctuations in a region of size R are not screened. Therefore, for a given electron density n_e , we only need to take into account fluctuations in regions of size $R < R_c = n_d^{1/2} / \pi^{1/2} n_e$. Thus the upper limit of integration over r in Eq. (4) can be replaced with $R_c = n_d^{1/2} / \pi^{1/2} n_e$; consequently

Equation (6) yields two simple limiting regimes for the relevance of screening effects:

$$\langle \delta\phi^2 \rangle = \frac{n_d e^2}{8\pi\kappa^2 \epsilon_0^2} \times \begin{cases} \ln \left(\frac{2d}{\lambda} \right), & R_c \gg 2d \gg \lambda \\ \frac{1}{2} \ln \left(1 + \left(\frac{R_c}{\lambda} \right)^2 \right), & 2d \gg R_c, \lambda \end{cases}. \quad (7)$$

The physical picture behind Eq. (7) is as follows. The metal electrode screens potential fluctuations on a length scale of d . Thus, if the fluctuations of the dopant density give a screening radius R_c that is larger than d , we may ignore the screening effects of a finite electron density n_e . For the devices we are interested in, the important limit is generally where d is considerably larger than λ , although R_c may be of the same order as, or greater than d at very low electron densities. We also note that R_c cannot fall below $n_d^{-1/2}$, since the Gaussian approximation [Eq. (2)] that we used to determine it will no longer be valid.

Let us now estimate the spatial dimensions of the electron droplets localized in the minima of the smoothly fluctuating 2DEG potential. We first do this for moderate electron densities, for which we can assume $2d \gg R_c$, to illustrate our logic, and then also consider the situation $2d \sim R_c$, where one has to deal with Eq. (6) numerically.

From Eq. (7), it is clear that the confining potential increases as the distance to the δ -layer, λ , is decreased. Nevertheless, the kinetic energy cost of electron confinement in the z -direction means that the localization length in the z -direction does not vanish. We assume that the electron wavefunction is localized in the z -direction in the GaAs substrate with a characteristic lengthscale z_0 . Hence, the kinetic energy of the electron is of the order of $n^2 \hbar^2 \pi^2 / (2mz_0^2)$, (n is a natural number) and the typical distance of the electron from the dopant layer is of the order of $\lambda + z_0$. The potential fluctuation expression in Eq. (7) then needs to be modified:

$$e\sqrt{\langle \delta\phi^2 \rangle} = \frac{e^2 n_d^{1/2}}{4\sqrt{\pi\kappa\epsilon_0}} \left\{ \ln \left[1 + \left(\frac{R_c}{\lambda + z_0} \right)^2 \right] \right\}^{1/2}. \quad (8)$$

We now minimize the total energy with respect to $z_{0,n}$ to get the binding energy E_n for the n^{th} sub-band,¹⁴ where

$$E_n = \frac{\hbar^2 \pi^2 n^2}{2mz_{0,n}^2} - \frac{n_d^{1/2} e^2}{4\sqrt{\pi\kappa\epsilon_0}} \left\{ \ln \left[1 + \left(\frac{R_c}{\lambda + z_{0,n}} \right)^2 \right] \right\}^{1/2}. \quad (9)$$

n_e (cm $^{-2}$)	R_c	E_1 (K)	E_2 (K)	$z_{0,1}$	R_p	Δ (K)	ξ
10^{11}	56	-69	-29	49	52	45	17
5×10^{10}	113	-133	-77	43	50	47	9
2×10^{10}	282	-202	-141	42	50	47	6.5
10^{10}	564	-221	-159	42	50	47	6

Table I: Values of the screening radius R_c , the bound state energies E_1 and E_2 , and the penetration distance for the lowest sub-band $z_{0,1}$ in the GaAs layer for different values of electron density n_e . Also shown are the droplet sizes R_p , the highest energy Δ of the electrons occupying a droplet, and the localization lengths ξ for inter-droplet tunneling. The lengths R_c , $z_{0,1}$, R_p and ξ are all in units of nanometers.

A bound state is always possible with such a potential because while the kinetic energy decreases as $1/z_{0,n}^2$, the magnitude of the potential energy decreases only as $1/z_{0,n}$. The minimization leads to the following transcendental equation for $z_{0,n}$:

$$z_{0,n}^3 = \frac{n^2 \pi^{\frac{3}{2}} a_B}{n_d^{\frac{1}{2}}} (\lambda + z_{0,n}) \left[1 + \left(\frac{\lambda + z_{0,n}}{R_c} \right)^2 \right] \times \left\{ \ln \left(1 + \left(\frac{R_c}{\lambda + z_{0,n}} \right)^2 \right) \right\}^{\frac{1}{2}}. \quad (10)$$

Eq. (10) gives good results when $2d \gg R_c$. For values of the electron density where this condition is not well-satisfied, then in Eq. (9), the more accurate expression for potential fluctuations, Eq. (6) should be used. Table I shows the numerically calculated values of E_1 , E_2 , $z_{0,1}$ and $z_{0,2}$ using Eq. (6), with λ replaced by $\lambda + z_0$, for the potential fluctuations.

The 2DEG electrons fill the lowest sub-band first and the second sub-band does not begin to be populated until the most energetic electron in the lower level reaches E_2 . The basic result of this analysis is that droplets can form due to electrons filling the minima of the screened disorder potential.

We now consider the dimension of the droplets in the plane of the 2DEG. The following arguments are valid for both $z_0 > \lambda$ and $z_0 < \lambda$. In a region of size $R \ll R_c$, the charge density fluctuation is of the order of $n_d^{1/2}/\pi^{1/2}R \gg n_e$. The electrons begin filling these small but deep regions first in an attempt to screen the strongest charge fluctuations and the density $n_{e,\text{local}} = n_d^{1/2}/\pi^{1/2}R$ of electrons in these droplets will be much larger than the mean 2DEG electron density n_e . However, since the kinetic energy rises with confinement, this limits the density from becoming too large, since to high a density would prevent the formation of bound states. With an electron density of $n_{e,\text{local}}$, correlations of the potential beyond the length scale R will get screened. Using the arguments we employed for $\langle \delta\phi^2 \rangle$ earlier, we can similarly say that the potential fluctuation with an

electron density of $n_{e,\text{local}}$ will be of the order of

$$\left(\frac{e^2 n_d^{1/2}}{4\sqrt{\pi}\kappa\epsilon_0} \right) \left\{ \ln \left[1 + \left(\frac{R}{\lambda + z_0} \right)^2 \right] \right\}^{\frac{1}{2}}. \quad (11)$$

In an electron droplet of size R_p , the kinetic energy of the electron occupying the highest state in the droplet will be of the same order as the potential energy fluctuation. If R_p is small compared to $\lambda + z_0$ (we shall see shortly that this is the case), the local fluctuation, Eq. (11) is a linear- R confinement. For such a confinement, the virial theorem suggests that the kinetic energy should be half of the potential energy. For the lowest sub-band, $n = 1$, we have

$$\frac{\hbar^2 k_{\text{max}}^2}{2m} = \frac{1}{2} \times \frac{e^2 n_d^{1/2}}{4\sqrt{\pi}\kappa\epsilon_0} \left[\ln \left(1 + \left(\frac{R_p}{\lambda + z_{0,1}} \right)^2 \right) \right]^{\frac{1}{2}}. \quad (12)$$

It should be noted that we can only make an order of magnitude comparison, as obtaining the exact magnitude of the screened Coulomb fluctuations where the electrons are pooled is beyond the scope of our discussion. To estimate the wavevector k_{max} we note that the droplet is effectively two-dimensional since motion deep into the GaAs substrate is not possible. Equating the number of droplet eigenstates, $(k_{\text{max}} R_p)^2/2$, with the charge fluctuation N_e in the droplet, $N_e = \pi^{1/2} n_d^{1/2} R_p$, (the number of electrons screening the potential fluctuation on a length scale R), we have $k_{\text{max}}^2 = 2n_d^{1/2} \pi^{1/2}/R_p$. Using this estimate for k_{max} in Eq. (12), we arrive at the condition

$$\frac{a_B}{R_p} = \frac{1}{2} \left[\ln \left(1 + \left(\frac{R_p}{\lambda + z_{0,1}} \right)^2 \right) \right]^{\frac{1}{2}}, \quad (13)$$

and when we specialize to the case $\lambda + z_{0,1} \gg a_B$, the droplet condition, Eq. (13) gives

$$R_p \sim R_{p,1} = \sqrt{2a_B(\lambda + z_{0,1})}, \quad (14)$$

as the size of the droplet in the lowest sub-band. We note that in Ref. 14 the form of the potential energy used to estimate R_p was for the $\lambda \ll R$ limit, however, the conclusion of the analysis was that $R_p \sim \lambda$. This invalidates the original assumption and Eq. (13) should be used instead. Equation (14) gives for $n_e = 5 \times 10^{10}$ cm $^{-2}$ and $z_{0,1} \simeq 43$ nm, $R_{p,1} \simeq 43$ nm. This compares well with the numerical estimate, $R_p \simeq 50$ nm (see Table I).

The estimate for R_p can be further improved by noting that z_0 itself varies with R_p . Physically, the confining potential is weaker at smaller values of R_p , therefore z_0 increases as R_p is decreased. This effect will lead to an enhancement of R_p . For this purpose, one needs to minimize Eq. (9) for z_0 as a function of $R_p \ll (\lambda + z_0)$,

and then use the R_p -dependent z_0 in Eq. (13) to obtain the droplet size. We have not followed this quantitatively more accurate but tedious procedure. Many of our quantitative estimates will be affected by our inability, in the present paper, to get a better estimate for R_p . However our qualitative predictions, and in particular, the dependence of quantities on experimental parameters is not affected. In our quantitative estimates we will, for the sake of greater accuracy, use the numerically computed values rather than the analytic expressions that are strictly valid for $2d \gg R_c$.

The density of electrons in the droplets, $n_{e,\text{local}}$, is a little greater than the average electron density, n_e . For example, for $n_e = 5 \times 10^{10} \text{ cm}^{-2}$, we have $n_{e,\text{local}} = n_d^{1/2}/\pi^{1/2}R_p \simeq 1.1 \times 10^{11} \text{ cm}^{-2}$. The local variation in the electron density is due to the movement of charge in the potential landscape from the “hills” to the “lakes”. The number of electrons in a droplet, $N_e = \pi^{1/2}n_d^{1/2}R_p$, is only weakly dependent on the average electron density through z_0 . Extra electrons are accommodated in the 2DEG through increasing the density of droplets. The separation between the droplet centers,

$$l_{ip} = 2(n_d^{1/2}R_p/\pi^{1/2}n_e)^{1/2} = 2\sqrt{R_cR_p}, \quad (15)$$

decreases with increasing average electron density n_e . We note that a previous discussion of droplet formation in 2DEGs¹⁴ states that $l_{ip} = R_c$ for the purposes of calculating the conductivity. We correct that statement here, as our analysis makes clear that this is not the case for the regimes of interest.

Next we discuss the height of the barrier separating two droplets, E_{barrier} . This barrier is not simply the size of the fluctuation from the bottom of the potential well, $e\sqrt{\langle\delta\phi^2\rangle}$, which is what one would find for “empty” potential wells. Instead we need to consider the occupation of the wells, and hence E_{barrier} is given by the difference between the magnitude of the binding energy E_n for confinement in the z direction and $\Delta = \hbar^2k_{\text{max}}^2/2m = \hbar^2\pi^{1/2}n_d^{1/2}/(mR_p)$, the highest energy for the electrons occupying a well, reckoned from the bottom of the well. The inter-droplet barrier height E_{barrier} is hence given by $E_{\text{barrier}} = |E_1| - \Delta$. Additionally, the typical number of electrons in a droplet is $N_e = \pi^{1/2}n_d^{1/2}R_p \simeq 9$ for $n_e = 5 \times 10^{10} \text{ cm}^{-2}$ and $R_p = 50 \text{ nm}$. Thus the mean level spacing in the droplets, $\delta \sim \Delta/N_e = \hbar^2/(mR_p^2) \simeq 5 \text{ K}$. As Δ is typically of the order of the sub-band spacing $|E_1 - E_2|$, the second sub-band in the z direction is also likely to be populated to a certain degree, although at low enough electron densities and temperatures, this should not be a major concern, and due to the uncertainty of our estimates, we shall assume that only the lowest sub-band is populated. We do not expect this to significantly alter our conclusions. The distance r between the surfaces of two neighboring droplets is

$$r = l_{ip} - 2R_p = 2(\sqrt{R_cR_p} - R_p). \quad (16)$$

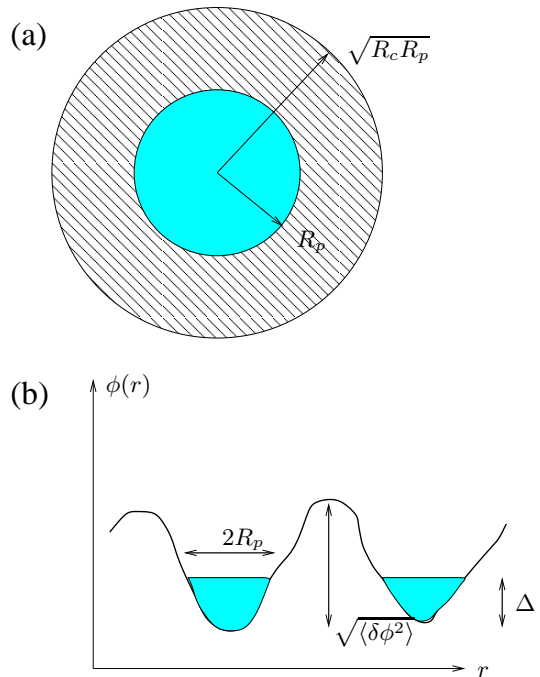


Figure 2: Schematic picture of droplets. (a) A typical droplet (shown in solid shading) has a radius of the order of the distance λ between the 2DEG and the δ -layer. For a dopant density n_d , the total number of electrons in the droplet is $N_e \sim n_d^{1/2}R_p$. For an average 2DEG electron density n_e , the “catchment area” (shown in line shading) is $\sim n_d^{1/2}R_p/n_e = R_cR_p$. Thus the inter-droplet distance is of the order of $\sqrt{R_cR_p}$. (b) Cross-section of energy profile between droplets. The electrons fill up to an energy Δ from the bottom of the potential wells. The magnitude of the potential fluctuations is $|E_1| \sim e\sqrt{\langle\delta\phi^2\rangle} \gg \Delta$.

The localization length for inter-droplet tunneling can be obtained from the size of the barrier,

$$\xi = \hbar/\sqrt{2mE_{\text{barrier}}} = \hbar/\sqrt{2m(|E_1| - \Delta)}. \quad (17)$$

Table I lists the calculated values of Δ and ξ for different electron densities. Note that the localization length here is of the order of the Bohr radius in GaAs. This should be regarded as a coincidence.

C. Summary

In the previous section (Sec. II B), we showed that for low electron density delta doped heterostructures that give rise to 2DEGs, it is very natural to expect that electrons will organize themselves into droplets of charge, centered on the minima of the screened disorder potential, for a quite reasonable range of parameters. The important length and energy scales of the droplets that relate to the transport properties of the device are the inter-droplet spacing, and the energy barriers between droplets, as summarized in Fig. 2.

III. MAGNETOTRANSPORT

In this section we consider several aspects of magneto-transport. In particular, we first consider the regime of low magnetic fields, where, due to quantum interference effects, one generically expects negative magnetoresistance, and we then move to higher magnetic fields, where one expects positive magnetoresistance due to shrinking of the localization length with increasing magnetic field. Our results are in good agreement with experiment.

A. Small fields: negative magnetoresistance

At small magnetic fields, many 2DEGs show negative magnetoresistance, i.e. the resistance decreases with increasing magnetic field, which is generically due to the magnetic field suppressing quantum interference of different electron paths. The samples in Ref. 10 show quadratic negative magnetoresistance at small fields:

$$[\mathcal{R}(B) - \mathcal{R}(0)]/\mathcal{R}(0) = -(B/B_c)^2, \quad (18)$$

with $B_c \simeq 0.15$ T. In the same magnetic field range, the temperature dependence of the resistance obeys an Arrhenius law for temperatures greater than about 1 K.

There are two contexts in which negative magnetoresistance in insulators has been studied in the literature. The first is hopping conductivity in dirty semiconductors, and the second is tunneling between droplets of charge, similarly to the picture outlined in the previous section.

In dirty semiconductors, electrical conductivity occurs due to hopping between different impurity sites and negative magnetoresistance is a consequence of suppression of the destructive interference of the Aharonov-Bohm phases acquired different trajectories.^{25,26,27} Such a theory gives a negative magnetoresistance $\propto |B|$, the perpendicular magnetic field, for fields such that $(BD^{3/2}\xi^{1/2})/\phi_0 > e^{-D/\xi}$.^{26,27} [ξ is the localization length, $\phi_0 = h/e$ is the flux quantum, and D is the hopping distance.] For smaller magnetic fields the negative magnetoresistance is quadratic in B . If we use the value of ξ and $D = r$ from our droplets scenario, this criterion suggests the negative magnetoresistance will be quadratic in the applied field up to $B \sim 0.2$ T for $n_e = 5 \times 10^{10} \text{ cm}^{-2}$.

In our case, the physical situation is somewhat different because instead of hopping between impurity sites as in a dirty semiconductor, the electrons in the 2DEG hop between droplets. The distance between the centers of neighboring droplets, $l_{ip} = 2\sqrt{R_c R_p}$, is comparable with the droplet diameter $2R_p$, unlike a dirty semiconductor where the electrons are localized at point-like impurity sites. This situation was studied in Ref. 21 where it was shown that the resistance between two droplets behaves as

$$\frac{\mathcal{R}(B)}{\mathcal{R}(0)} = e^{(B/B_0)^2} \frac{1}{\cosh^2(B/B_1)}, \quad (19)$$

$n_e (\text{cm}^{-2})$	$B_0 (\text{T})$	$B_1 (\text{T})$	$D (\text{nm})$	$\alpha (\text{T}^{-2}),$ $D = (3l_{ip}^2 r/4)^{1/3}$	$\alpha (\text{T}^{-2}),$ $D = r$
10^{11}	1.45	0.22	33	0.48	9.6×10^{-4}
5×10^{10}	0.42	0.12	95	5.7	0.84
2×10^{10}	0.19	0.05	180	29	13
10^{10}	0.10	0.024	271	94	62

Table II: Magnetic fields B_0 and B_1 as defined in Eq. (20) for different electron densities. These fields determine the crossover between negative and positive magnetoresistance. Also shown are the inter-droplet tunneling distance $D = (3l_{ip}^2/4)^{1/3}$ and α , both of which appear in magnetoresistance expressions in Sec. III B. $D = (3l_{ip}^2 r/4)^{1/3}$ is the tunneling distance obtained by reconciling Eqs. (19) and (20) with Eq. (21). Values of α are also shown for comparison by assuming the tunneling distance D is equal to the distance r between the surfaces of neighboring droplets.

where B_0 and B_1 have the following approximate expressions in terms of our droplet parameters:

$$\begin{aligned} B_0 &\sim \phi_0 / (\pi y_0 l_{ip}), \\ B_1 &\sim 2\phi_0 / (\pi l_{ip}^2), \end{aligned} \quad (20)$$

and we note that $l_{ip} = 2\sqrt{R_c R_p}$, and we estimate that the spread of the wavefunction under the barrier in the direction perpendicular to the tunneling is $y_0 \sim \sqrt{\xi r}$. Both B_0 and B_1 are determined by the field for which a flux quantum is enclosed within an area that is of significance in the droplet picture. B_0 is the field that encloses a flux quantum in an area of the order of the area enclosed by the electron wavefunction tunneling under the barrier. B_1 is the field that encloses a flux quantum in an area of the order of the ‘‘catchment region’’. [See Fig. 2]. Physically, B_1 is the field below which interference effects are significant. If $B_0 > B_1$, then at small fields, the magnetoresistance will be negative as in Eq. (18), with $B_c^{-2} = B_1^{-2} - B_0^{-2}$. Table II lists B_0 and B_1 for various electron densities.

For $n_e = 5 \times 10^{10} \text{ cm}^{-2}$ we can infer from Table II that $B_c \simeq 0.12$ T, which is close to the experimentally observed $B_c \simeq 0.15$ T.^{9,10} We note that recent experiments on a quantum dot lattice²⁸ also displayed negative magnetoresistance that appeared to be well explained by the Glazman and Raikh approach.

The positive magnetoresistance in Eq. (19) arises from the shrinking of the localization length in a strong magnetic field. This has been extensively studied in the contest of dirty semiconductors. In dirty semiconductors, the $e^{(B/B_0)^2}$ dependence of magnetoresistance is predicted to cross over to a e^{B/B_2} dependence at a high enough field. This is seen in the experiments we are discussing too, while Eq. (19) makes no such prediction. The high field data are better described by Shklovskii’s expressions (see Sec. III B) for magnetoresistance for tunneling in dirty semiconductors.^{22,23} This is the subject of the following section.

B. Larger fields: positive magnetoresistance

The important length scale for magnetotransport in the regime of magnetic fields where interference effects are negligible, is the length scale of the “unit cell” of the droplet array. What we mean is the regime $l_{ip} > 2l_0$, where $l_{ip} = 2\sqrt{R_c R_p}$ is the separation between the centers of neighboring droplets, and $l_0 = \sqrt{\hbar/eB}$ is the magnetic length.

Now, it is well known from Refs. 22 and 23 that once the magnetic field is large enough, $B > B_1$, so that quantum interference effects are negligible in comparison with the positive magnetoresistance arising from the reduction of the localization length, the magnetoresistance takes the form

$$\frac{\mathcal{R}(B)}{\mathcal{R}(0)} \sim e^{\alpha B^2}, \quad (21)$$

in the field range

$$\frac{2\phi_0}{\pi l_{ip}^2} < B \ll \frac{\hbar}{e\xi D}. \quad (22)$$

In Eq. (21), with D the typical tunneling distance as before, α is given by

$$\alpha = \frac{D^3 \xi e^2}{3\hbar^2}. \quad (23)$$

If we take α to be determined from Eq. (19), then we can identify $\alpha = B_0^{-2}$, and the tunneling distance

$$D = [3l_{ip}^2 r/4]^{1/3}. \quad (24)$$

The upper limit for B for the validity of Eq. (21), $\hbar/(e\xi D)$, is about 0.8 T for $n_e = 5 \times 10^{10} \text{cm}^{-2}$. The quantitative estimate for α is very sensitive to r and l_{ip} which limits its reliability. Using the extrapolation of Eq. (19), one should observe

$$\alpha = \frac{A}{n_e^{3/2}} \left(1 - \frac{R_p^{1/2}}{R_c^{1/2}} \right) \sim \frac{A}{n_e^{3/2}}, \quad (25)$$

where $A = 2n_d^{3/4} R_p^{3/2} \xi e^2 / (\pi^{3/4} \hbar^2)$. A similar calculation, taking Shklovskii's expression for α , with $D = r$, also yields $\alpha \simeq A'/n_e^{3/2}$, where A' and A differ by a factor of order unity but have the same dependence on n_d , R_p , and ξ . In both scenarios, the tunneling distance D increases as $1/n_e^{1/2}$ as the electron density decreases, indicating that the n_e dependence of α is robust; additionally, α is seen to be independent of temperature. This is exactly what was observed in Ref. 10, although in that case the $n_e^{-3/2}$ dependence of α was ascribed to a Wigner crystal (or a charge density wave) where the density of localized states is expected to be equal to the density of electrons.

We note that for the experimental parameters in Ref. 9, there is quantitative agreement between our prediction for α and the observed behavior. In particular, considering D as given by Eq.(24), we have for $n_e \simeq 10^{11} \text{cm}^{-2}$, $\alpha \simeq 1.5 \times 10^{22} \text{m}^{-3} \text{T}^{-2} / n_e^{3/2}$, and if $n_e \simeq 5 \times 10^{10} \text{cm}^{-2}$, $\alpha \simeq 6.4 \times 10^{22} \text{m}^{-3} \text{T}^{-2} / n_e^{3/2}$. These values are about an order of magnitude of the values quoted in Ref. 9, however, we note as in Sec. II B that one of the main impediments to greater quantitative comparison with experiment is an inability to get a better estimate for R_p , which in turn affects our estimate of ξ . If one assumes that the tunneling distance is equal to the distance between the neighboring droplet surfaces, $D = r$, then one obtains for $n_e \simeq 5 \times 10^{10} \text{cm}^{-2}$ that $\alpha \simeq 9.4 \times 10^{21} \text{m}^{-3} \text{T}^{-2} / n_e^{3/2}$, which is closer to experiment.

In our droplets picture such a behavior of D arises due to the n_e dependence of the typical droplet spacing, and the n_e dependence of α in Eq. (25) is one of our main results.

The expression for the magnetoresistance, Eq. (21), is valid when $D \ll l_0^2/\xi$, and for higher magnetic fields where $D \gg l_0^2/\xi$, (or equivalently, $B \gg \frac{\hbar}{e\xi D}$) it crosses over to another regime,^{22,23}

$$\frac{\mathcal{R}(B)}{\mathcal{R}(0)} \sim e^{B/B_2}, \quad (26)$$

where

$$B_2 = \frac{\hbar}{eD^2}. \quad (27)$$

In this regime of magnetic field, the result of Ref. 21 presented in Eq. (19) is no longer valid. Note also that the magnetoresistance expression, Eq. (26), rather than Eq. (21) or Eq. (19), describes the correct behavior as the electron density is decreased. Our estimate for B_2 is 0.07 T when $D \simeq 95 \text{nm}$. In the experiments,¹⁰ a crossover from a quadratic to a linear magnetic field dependence (in the exponent) has been observed, and it is in qualitative agreement with the expected crossover $B \sim \frac{\hbar}{e\xi D} \sim 0.8 \text{T}$, for the parameters mentioned above. Again, we are able to predict the dependence of this field on n_e ; at low electron density,

$$B_2 \propto \frac{\hbar n_e}{e n_d^{3/2} R_p}.$$

This implies that the resistance should increase more quickly as a function of magnetic field in samples with lower n_e , which is observed in experiment.¹⁰

The picture we have discussed in this section, is one in which the transport at increasing magnetic fields is dominated by barriers between droplets. As we have seen, the barrier transparency drops exponentially as the magnetic field is increased. This suggests that for large enough magnetic fields, individual droplets will be relatively well isolated from each other, and that one can think of the

droplets as an irregular array of quantum dots. This has further implications for transport which we will discuss in future work.²⁹

IV. DISCUSSION

The picture of electron droplets we have discussed here provides an appropriate framework for describing the phenomenology of the recent experiments in Ref. 10. As we outline in Sec. III B, we are able to use the droplet picture to make both qualitative and quantitative comparisons with experiment. [We note that some of the quantitative agreement may be fortuitous, however the dependence on 2DEG parameters should not be.] Importantly, we are able to reproduce the dependence of the magnetoresistance on the electron density. This strong agreement with experiment, in conjunction with our analysis of the electronic environment in the 2DEG, strongly implies that a picture of electronic droplets is more suitable to describe these, and similar experiments than a charge density wave scenario.

One point that we did not discuss quantitatively, was how the non-linear screening is affected by the presence of a magnetic field. There has been some discussions of screening 2D electrons in a disordered potential in a magnetic field,^{18,19,20} but this has tended to focus on the regime in which disorder is not too strong. We regard this as a very interesting problem that merits further investigation; however, we note that experiment appears to provide some of the solution (hence our neglect of the issue here). Measurements of localized states in the quantum Hall regime⁴ that support a dot-like picture at low densities, find that the local electronic compressibility is essentially independent of the magnetic field, supporting our assumptions here.

In our analysis we have assumed that the dopants are completely ionized. The degree of ionization is determined by the internal field at the GaAs-AlGaAs junction, the external gate voltage V_g , and the temperature T_0 at which the electron distribution over the dopants is frozen. Suppose the conditions are such that the donors are not completely ionized. In particular, consider that the gate voltage V_g is zero and that the electron distribution over the dopants is frozen at a nonequilibrium temperature T_0 which is less than the RMS potential fluctuation in the δ -layer. This case has been studied, for example, in Ref. 24, where the authors calculate the dopant atoms' correlator,

$$D(\mathbf{r} - \mathbf{r}') = \langle n(\mathbf{r})n(\mathbf{r}') \rangle - \langle n \rangle^2, \quad (28)$$

using a path integral approach. The probability of a fluctuation $c(\mathbf{r}) = n(\mathbf{r}) - \langle n \rangle$ is proportional to $\exp(-\Phi[c])$, where

$$\Phi[c] = \frac{1}{2n_d} \int d\mathbf{r} c^2(\mathbf{r}) + \frac{1}{k_B T_0} \int d\mathbf{r} d\mathbf{r}' c(\mathbf{r}) G(\mathbf{r} - \mathbf{r}') c(\mathbf{r}'); \quad (29)$$

$G(\mathbf{r} - \mathbf{r}')$ is the interaction energy of two electrons in the δ -layer:

$$G(\mathbf{r} - \mathbf{r}') = \frac{e^2}{4\pi\epsilon_0\kappa} \left[\frac{1}{|\mathbf{r} - \mathbf{r}'|} - \frac{1}{|\mathbf{r} - \mathbf{r}'|^2 + 4(d - \lambda)^2} \right]. \quad (30)$$

The dopant atoms' correlator is then given by

$$D(\mathbf{r} - \mathbf{r}') = \left[\int Dc c(\mathbf{r})c(\mathbf{r}') e^{-\Phi[c]} \right] / \left[\int Dc e^{-\Phi[c]} \right] \quad (31)$$

Its Fourier transform $D(\mathbf{q})$ can be shown to be

$$D(q) = \frac{n_d q}{q + q_0 [1 - \exp[-2q(d - \lambda)]]}, \quad (32)$$

where $q_0 = n_d e^2 / (2\epsilon_0 \kappa k_B T_0)$ is the reciprocal Debye radius. In Ref. 24, $T_0 = 100\text{K}$; for this value we may assume that $q_0 \gg q$. In the absence of dopant correlation, we have $D(q) = n_d$ as in Eq.(2). For $q(d - \lambda) \ll 1$, the correlator $D(q)$ approaches a constant value,

$$D(q) \approx n_0 = \frac{\epsilon_0 \kappa k_B T_0}{e^2 (d - \lambda)}. \quad (33)$$

We estimate $n_0 = 2.5 \times 10^9 \text{cm}^{-2} = 2 \times 10^{-3} n_d$. Note that the correlator in Eq.(33) has the same form as the uncorrelated case, Eq.(2), except that the dopant density n_d is replaced by a smaller effective dopant density n_0 . This implies that the potential fluctuations in the 2D electron layer (see Eq.(eq:meansqpotlimits)) are reduced, and the characteristic length scale beyond which the donor charges are uncorrelated is much larger. The R_c corresponding to the reduced density is smaller than the original value by a factor of 20. Thus a much smaller electron density in the 2D layer suffices to screen the potential fluctuations from correlated dopants. The puddle size R_p is relatively less affected by dopant correlation. Lower values of R_c will take the system closer to metallicity since the puddles will merge once R_c becomes smaller than R_p . In the experiments we have studied, the observations are better explained by assuming a complete ionization of the donors.

We also find it worthwhile to say a few words on the effect of sample width on the puddles scenario. This has been studied numerically, for example, in Ref. 15. The conclusion is that a reduction of the sample width diminishes the effectiveness of screening of the potential fluctuations due to the dopant atoms, and the resulting enhanced potential fluctuations make puddle formation easier. In fact, the inter-puddle separation will increase. For studying ballistic transport in quantum wires, one should must work in a regime where the potential fluctuations are lower. This can be made possible by working with, say, gate voltages V_g where the dopants are incompletely ionized.

It is interesting to view our results in the broader context of other physical phenomena observed in systems

with nanoscale electronic disorder. This includes other effects observed in low density delta-doped 2DEGs, and in systems such as the underdoped cuprates.⁶ The picture of droplets of charge that merge as the doping is increased may also have relevance to the 2D metal-insulator transition.^{30,31,32} It is interesting to note that experiments on the insulating side of this transition have noted small jumps in the chemical potential as a function of n_e ,³³ and we speculate that these small jumps may be relevant to the small amplitude oscillatory behavior of α as a function of n_e observed in Refs. 9 and 10. We note that our discussions here also lead to a plausible explanation of recent observations of a zero-bias anomaly in insulating 2DEG samples at low magnetic fields.^{12,34} This zero-bias anomaly might be due to exchange interactions between electrons on two closely coupled droplets having a Kondo effect similar to that observed in double quantum dot systems.³⁵ In the limit of higher density and larger magnetic fields, our picture should evolve continuously into existing droplet-based transport theory for the quantum Hall regime.^{36,37} It would be interesting to

try to connect our work with this scenario. Finally, our analysis of strong disorder in delta-doped heterostructures could perhaps also be extended to a recent interesting proposal for creating strongly correlated electron systems by modulation doping near a heterojunction of two Mott insulators.³⁸

Acknowledgments

The authors thank David Khmelnitskii, and Ben Simons for illuminating discussions, and in particular thank Nigel Cooper for suggesting the idea of charge droplets in the Ghosh experiments. We especially thank Arindam Ghosh and Matthias Baenninger for many interesting discussions, for critically reading this manuscript and for sharing their unpublished data with us. V.T. acknowledges the support of Trinity College, Cambridge, and TIFR, Mumbai, and M.P.K. acknowledges support from NSERC.

-
- ¹ D. C. Tsui, H. L. Stormer, and A.C. Gossard, Phys. Rev. Lett. **48**, 1559 (1982).
- ² S. Ilani, A. Yacoby, D. Mahalu, and H. Shtrikman, Science **292**, 1354 (2001).
- ³ J. Martin, S. Ilani, B. Verdene, J. Smet, V. Umansky, D. Mahalu, D. Schuh, G. Abstreiter, and A. Yacoby, Science **305**, 980 (2004).
- ⁴ S. Ilani, J. Martin, E. Teitelbaum, J. H. Smet, D. Mahalu, V. Umansky, and A. Yacoby, Nature **427**, 328 (2004).
- ⁵ J. Wiebe, C. Meyer, J. Klijn, M. Morgenstern, and R. Wiesendanger, Phys. Rev. B **68**, 041402(R) (2003).
- ⁶ S. H. Pan, J. P. O'Neal, R. L. Badzey, C. Chamon, H. Ding, J. R. Engelbrecht, Z. Wang, H. Eisaki, S. Uchida, A. K. Gupta, K.-W. Ng, E. W. Hudson, K. M. Lang, and J. C. Davis, Nature **413**, 282 (2001); K. M. Lang, V. Madhavan, J. E. Hoffman, E. W. Hudson, H. Eisaki, S. Uchida, and J. C. Davis, Nature **415**, 412 (2002); K. McElroy, J. Lee, J. A. Slezak, D.-H. Lee, H. Eisaki, S. Uchida, and J. C. Davis, Science **309**, 1048 (2005).
- ⁷ S. Nakatsuji, V. Dobrosavljevic, D. Tanaskovic, M. Minakata, H. Fukazawa, and Y. Maeno, Phys. Rev. Lett. **93**, 146401 (2004); T. Park, Z. Nussinov, K. R. A. Hazzard, V. A. Sidorov, A. V. Balatsky, J. L. Sarrao, S. W. Cheong, M. F. Hundley, J.-S. Lee, Q. X. Jia, and J. D. Thompson, Phys. Rev. Lett. **94**, 017002 (2005).
- ⁸ E. Dagotto *et al.*, Phys. Reports **344**, 1 (2001); N. Mathur and P. B. Littlewood, Phys. Today **56**, 25 (2003); V. B. Shenoy, T. Gupta, H. R. Krishnamurthy, and T. V. Ramakrishnan, cond-mat/0606660.
- ⁹ M. Baenninger, A. Ghosh, M. Pepper, H. E. Beere, I. Farrer, P. Atkinson, and D. A. Ritchie, Phys. Rev. B **72**, 241311(R) (2005).
- ¹⁰ M. Baenninger *et al.* unpublished.
- ¹¹ A. Ghosh, M. Pepper, H. E. Beere, and D. A. Ritchie, Phys. Rev. B **70**, 233309 (2004).
- ¹² A. Ghosh, C. J. B. Ford, M. Pepper, H. E. Beere, and D. A. Ritchie, Phys. Rev. Lett. **92**, 116601 (2004).
- ¹³ A. Ghosh, M. Pepper, H. E. Beere, and D. A. Ritchie, J. Phys. Cond. Mat. **16**, 3623 (2004).
- ¹⁴ V. A. Gergel' and R. A. Suris, Zh. Eksp. Teor. Fiz. **75**, 191 (1978). [Sov. Phys. JETP **48**, 95 (1978)].
- ¹⁵ J. A. Nixon and J. H. Davies, Phys. Rev. B **41**, 7929 (1990).
- ¹⁶ J. Shi and X. C. Xie, Phys. Rev. Lett. **88**, 086401 (2002).
- ¹⁷ M. M. Fogler, Phys. Rev. B **69**, 121409(R) (2004); *ibid*, **69**, 245321 (2004); *ibid* **70**, 129902 (2004).
- ¹⁸ A. L. Efros, Solid State Commun. **67**, 1019 (1988).
- ¹⁹ A. L. Efros, Solid State Commun. **70**, 253 (1989).
- ²⁰ A. L. Efros, F. G. Pikus, and V. G. Burnett, Phys. Rev. B **47**, 2233 (1993).
- ²¹ M. E. Raikh and L. I. Glazman, Phys. Rev. Lett. **75**, 128 (1995).
- ²² B. I. Shklovskii and A. L. Efros, Zh. Eksp. Teor. Fiz. **84**, 811 (1983). [Sov. Phys. JETP **57**, 470 (1983)].
- ²³ B. I. Shklovskii, Fiz. Tekh. Poluprovodn **17**, 2055 (1983). [Sov. Phys. Semicond. **17**, 1311 (1983)].
- ²⁴ F. G. Pikus and A. L. Efros, Zh. Eksp. Teor. Fiz. **96**, 985 (1989). [Sov. Phys. JETP **69**, 558 (1989)].
- ²⁵ V. L. Nguen, B. Z. Spivak, and B. I. Shklovskii, JETP Lett. **41**, 42 (1985); Sov. Phys. JETP **62**, 1021 (1985).
- ²⁶ U. Sivan, O. Entin-Wohlman, and Y. Imry, Phys. Rev. Lett. **60**, 1566 (1988); O. Entin-Wohlman, Y. Imry, and U. Sivan, Phys. Rev. B **40**, 8342 (1989).
- ²⁷ W. Schirmacher, Phys. Rev. B **41**, 2461 (1990).
- ²⁸ A. Dorn, T. Ihn, K. Ensslin, W. Wegscheider, and M. Bichler, Phys. Rev. B **70**, 205306 (2004).
- ²⁹ V. Tripathi and M. P. Kennett, in preparation.
- ³⁰ S. V. Kravchenko, G. V. Kravchenko, J. E. Furneaux, V. M. Pudalov, and M. D'Iorio, Phys. Rev. B **50**, 8039 (1994); S. V. Kravchenko, W. E. Mason, G. E. Bowker, J. E. Furneaux, V. M. Pudalov, and M. D'Iorio, Phys. Rev. B **51**, 7038 (1995); S. V. Kravchenko, D. Simonian, M. P. Sarachik, W. Mason, and J. E. Furneaux, Phys. Rev. Lett. **77**, 4938 (1996); E. Abrahams, S. V. Kravchenko, and M.

- P. Sarachik, *Rev. Mod. Phys.* **73**, 251 (2001).
- ³¹ Y. Meir, *Phys. Rev. Lett.* **83**, 3506 (1999); *Phys. Rev. B* **61**, 16470 (2000); *Phys. Rev. B* **63**, 073108 (2001).
- ³² S. DasSarma, M. P. Lilly, E. H. Hwang, L. N. Pfeiffer, K. W. West, and J. L. Reno, *Phys. Rev. Lett.* **94**, 136401 (2005).
- ³³ S. Ilani, A. Yacoby, D. Mahalu, and H. Shtrikman, *Phys. Rev. Lett.* **84**, 3133 (2000).
- ³⁴ A. Ghosh, M. H. Wright, C. Siegert, M. Pepper, I. Farrer, C. J. B. Ford, and D. A. Ritchie, *Phys. Rev. Lett.* **95**, 066603 (2005).
- ³⁵ D. Goldhaber-Gordon, H. Shtrikman, D. Mahalu, D. Abusch-Magder, U. Meirav, and M. A. Kastner, *Nature* **391**, 156 (1998); S. M. Cronenwett, T. H. Oosterkamp, and L. P. Kouwenhoven, *Science* **281**, 540 (1998).
- ³⁶ N. R. Cooper and J. T. Chalker, *Phys. Rev. B* **48**, 4530 (1993).
- ³⁷ E. Shimshoni and A. Auerbach, *Phys. Rev. B* **55**, 9817 (1997).
- ³⁸ W.-C. Lee and A. H. MacDonald, *Phys. Rev. B* **74**, 075106 (2006).